2014

Automated Indoor RFID Inventorying using a Self-Guided Micro-Aerial Vehicle

Steven A. Parkison
University of Nebraska-Lincoln, sparkison@huskers.unl.edu

Eric T. Psota
University of Nebraska-Lincoln, epsota@unl.edu

Lance C. Pérez
University of Nebraska-Lincoln, lperez@unl.edu

Energy Conversion Congress and Exposition (ECCE), 2013 IEEE
Year: 2013
Pages: 3934 - 3940, DOI: 10.1109/ECCE.2013.6647222

Automated Indoor RFID Inventorying using a Self-Guided Micro-Aerial Vehicle

Steven A. Parkison, Eric T. Psota, and Lance C. Pérez
Department of Electrical Engineering, University of Nebraska-Lincoln
sparkison@huskers.unl.edu, epsota@unl.edu, lperez@unl.edu

***Abstract*—A Micro-Aerial Vehicle (MAV) system is presented for automated indoor inventorying using passive radio frequency identification (RFID). This system utilizes a combination of onboard sensing and processing in order to achieve flight stabilization, generate floor maps, and perform path planning. The proposed state estimation method along with a control feedback strategy are demonstrated to be sufficiently accurate for operation in the indoor environment and the proposed path planning technique is shown to be effective for guiding the MAV while it performs automated RFID scanning.**

I. Introduction

Micro-Aerial Vehicles (MAVs) can be used for a variety of consumer and industrial applications. While outdoor applications using MAVs are able to benefit from GPS and widely available outdoor maps, indoor applications pose several challenges to researchers. Enabling a MAV to fly safely and effectively indoors requires either a skilled pilot or a sophisticated combination of sensing hardware and control software. Automated MAVs are especially attractive for many indoor applications due to the potential for improved reliability and efficiency while removing human error. MAVs are also capable of navigating within areas that have difficult terrain, making them preferable to ground-based robotic platforms for search and rescue after disasters such as floods and earthquakes.

Systems capable of operating autonomously in the indoor environment must include methods that allow for real-time tracking of the MAV's location and effective obstacle avoidance. Advancements in the miniaturization of computing hardware and improvements in power-efficiency have allowed MAVs to do much of the processing onboard, while advances in sensor technology have made it possible to successfully achieve collision-free navigation and exploration in indoor environments [1].

The system proposed in this paper for automated RFID inventorying achieves full automation without the assistance of external sensing or processing. A customized high-payload Ascending Technologies Pelican quadrotor, shown in Figure 1, was chosen for this application. It includes an onboard computer with an Intel Core i7 quadcore processor and a 60 gigabyte solid state drive (SSD), a Hokuyo scanning laser rangefinder, a SkyeModule M9 RFID reader, and a downward facing ultrasonic depth sensor. This combination of onboard hardware allows the quadrotor to perform automated indoor flight while generating a map of the indoor space using the scanning laser rangefinder. The powerful onboard computer allows all processing to be done onboard, including determining which spaces are navigable and defining appropriate paths.

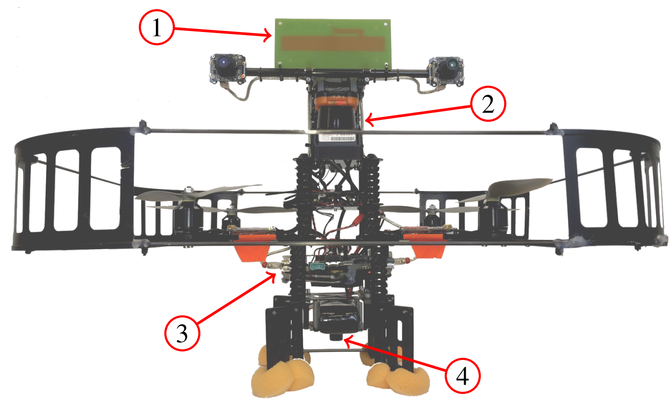

Figure 1: The Ascending Technologies Pelican quadrotor used for automated RFID inventorying. It is equipped with an (1) RFID antenna connected to an RFID reader, (2) scanning laser rangefinder, (3) onboard computer, and (4) downward facing ultrasonic depth sensor.

The system must be capable of performing a variety of tasks in order to be considered a capable solution for autonomous RFID inventorying. These tasks include flight control, path planning, and RFID scanning. This paper begins by presenting background and related research. Then, methods are introduced for performing the necessary tasks and, finally, experimental results are provided to verify the system's suitability for the proposed application.

II. Background

As the popularity of indoor MAVs grows, researchers have been forced to address the many challenges that come with autonomous mapping and navigation. These challenges include a limited sensing payload, indirect odometry, and fast dynamics [2]. More specifically, MAVs operating in indoor environments fly relatively close to physical boundaries, oftentimes introducing severe ground effects [3] [4]. Despite these difficulties, researchers have recently been able to successfully develop autonomous indoor systems for a variety of applications.

A commonly chosen platform for researchers interested in indoor autonomous MAVs is the quadrotor due to its dynamic flight capabilities, mechanical simplicity, and intuitive pitch/roll/yaw control [5]. There exists a wide range of platforms suitable for quadrotor research, from commoditized RC toys (e.g., WLtoys' V929 Beetle) and the popular Parrot AR.Drone to the customizable, high-payload Ascending Technologies Pelican. While smaller quadrotors are suitable for research related to controls and dynamics, they require external sensing and processing to track the quadrotor's position and orientation. One of the most common methods for external tracking is the Vicon system, which requires high-speed infrared cameras, light sources, and reflective markers mounted to the quadrotor [6], [7]. While the Vicon system solves the tracking problem for systems that operate in confined locations, it is not suitable for systems that operate in multi-room environments or those that are designed to operate in previously unvisited areas. For systems that lack external tracking and require all sensing and processing to be done onboard, a higher payload is required.

To achieve indoor mapping and navigation in previously unvisited areas, a quadrotor that includes a scanning laser rangefinder, an inertial measurement unit (IMU), and a Gumstix computer was presented in [8]. In addition, a mirror was used to direct a portion of the laser scan toward the ground so that the quadrotor could estimate its height. They were able to achieve autonomous indoor mapping and navigation using a novel multilevel simultaneous localization and mapping (SLAM) algorithm that combine scans at varying heights into a coherent 3D map. The resulting map allows the quadrotor to navigate over furniture without disrupting the onboard navigation, addressing one of the core challenges with using an inherently 2D scanning laser rangefinder for quadrotor navigation.

In [9], the authors attach both a scanning laser rangefinder and a Kinect to the top of a quadrotor in order to achieve multi-floor 2D SLAM. The authors also examined the possibility of using RGB cameras to achieve full 3D SLAM, but later chose 2.5D SLAM using a scanning laser rangefinder due to limited computational resources [10]. Expanding upon their previous work, they presented a stochastic differential equation-based method for path planning and exploration [1].

As discussed in the recent survey by Kendoul et al. [11], there has been growing interest in research related to autonomous MAVs. However, several challenges remain in terms of adapting the systems to specific applications, improving their overall safety, and achieving a level of reliability that is necessary for most industry and consumer applications.

III. Method

To allow automation of the MAV within the indoor environment, a control system was developed that uses a scanning laser rangefinder, an ultrasonic depth sensor, and an onboard inertial measurement unit. In the following sections, methods are presented for stabilizing and controlling the position and orientation of the quadrotor. To evaluate the accuracy of the proposed methods, ground truth position and orientation estimates have been obtained using an external camera to track a fiducial marker attached to the quadrotor. The fiducial marker tracking method, referred to as AprilTags [12], is capable of providing highly accurate, full six degree of freedom (6DOF) pose estimates in real time. Figure 2 shows the AprilTag used for visual tracking mounted to the top of the quadrotor.

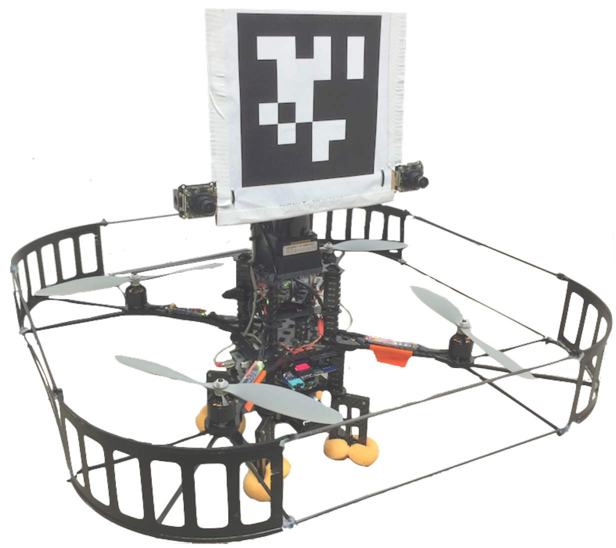

Figure 2: The quadrotor equipped with an AprilTag that is used for external tracking of the 3D position.

A. Altitude Control

The quadrotor is equipped with a Maxbotix MB1423 high-resolution USB ultrasonic sensor that is mounted to the bottom of the frame pointed toward the floor. This sonar depth sensor is capable of obtaining reliable distance measurements at a resolution of 1mm for objects between 300mm and 5000mm, which is sufficient for indoor applications where the ceiling height is often limited to 3000m or less. The sensing area is such that objects are generally detected within 10° to 15° of the direction that the device is pointed. It has been empirically determined that the cone-shaped spread of the sensing area is preferable to methods that use highly directional sensing because is ensures that the entire area of the quadrotor maintains is position safely above the nearest obstacle that exists below the quadrotor.

Figure 3 provides the results of an experiment in which altitude estimates were obtained using both AprilTag tracking and sonar. Two things are apparent when comparing the two estimates: 1) the difference in distance between peaks and valleys varies less with sonar and 2) the sonar measurements are delayed by $\approx$ 0.3 seconds. Although the proprietary method used by Maxbotix is not publicly available, we were able to closely approximate their sonar device's distance measurements by filtering the AprilTag measurements with a causal uniform filter that has width 0.6 seconds. A comparison between the filtered AprilTag measurements and sonar measurements is shown in Figure 3. Due to this delay, sonar was

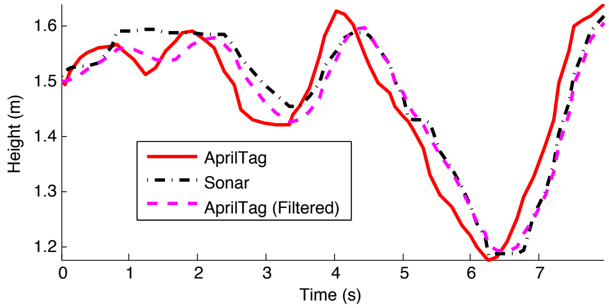

Figure 3: Altitude estimation using AprilTag tracking, sonar, and uniformly filtered AprilTag tracking.

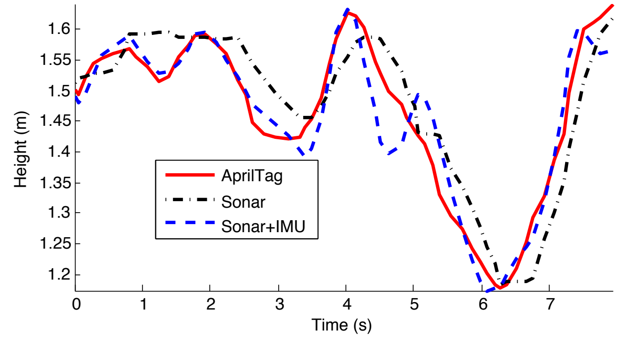

Figure 4: Altitude estimation using AprilTag tracking, sonar, and sonar combined with IMU data using predictive Kalman filtering.

determined through experiments to be insufficient by itself for altitude feedback control.

To overcome the sonar device's delay, Kalman filtering was used to combine measurements from sonar and the accelerometer included in the onboard IMU. The accelerometer measurements in the vertical direction, sampled every $\Delta t = 0.05$ seconds, were treated as measurements of the control input (thrust) and advance the state via the update equation

$$\mathbf{x}_t = \begin{bmatrix} 1 & \Delta t \\ 0 & 1 \end{bmatrix} \mathbf{x}_{t-\Delta t} + \begin{bmatrix} \frac{(\Delta t)^2}{2} \\ \Delta t \end{bmatrix} (a_t + w_t)$$

where $\mathbf{x}_t = [p_t, v_t]^T$ is the current state parameterized by the current position p_t and the current velocity v_t at time t, and w_t is noise affecting the measurement of the vertical acceleration a_t. Sonar measurements can be derived from the current state using

$$z_t = \begin{bmatrix} 1 & 0 \end{bmatrix} \mathbf{x}_t + v_t$$

where z_t is the height measurement obtained from sonar and v_t models the sonar noise. As shown earlier, the sonar measurements are delayed with respect to the true altitude of the quadrotor. Therefore, when operating the Kalman filter using the above model, it was necessary to delay the accelerometer readings by 0.3 seconds. The result is a Kalman filter estimate of the delayed state. The most recent accelerometer readings are then used to recursively advance the state estimate to the current time.

The affect of using the proposed method for predictive Kalman filtering can be seen in Figure 4. By incorporating the accelerometer data into altitude estimation, the delay is effectively removed. It can be seen that using this method to remove delay sometimes creates additional errors due to noise inherent in the accelerometer measurements, however, as long as the errors are limited in magnitude and duration they are easily tolerated by the proposed feedback control method.

The control loop used to stabilize the quadrotor's altitude is given in Figure 5, where p_g is the position goal, p_m is the position measured by Kalman filter state estimation, and u is the system input (thrust). The parameters k_p, k_i, and k_d are used to balance the influences of the proportional, integral, and derivative (PID) terms of the altitude error. In a similar fashion

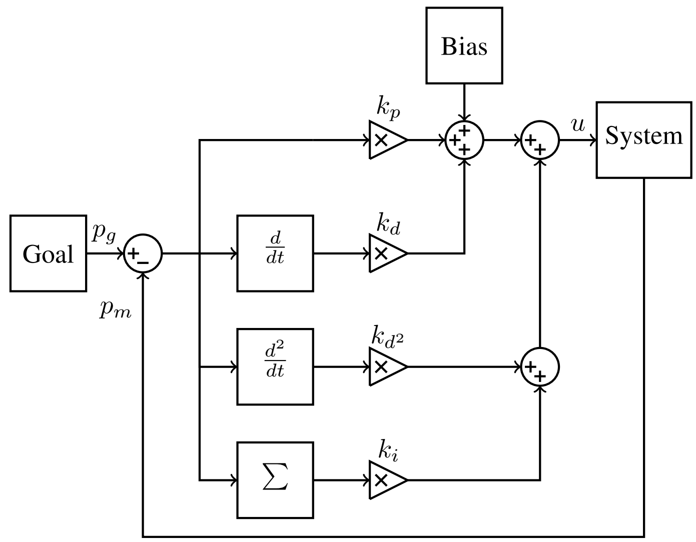

Figure 5: Control loop used to stabilize the quadrotor at the desired altitude.

to the method presented in [6], the integral operator (also referred to as an accumulator) quantizes the errors to -1 and +1 before summing. This was empirically found to provide more stable hovering than using unquantized errors. In addition to the traditional terms found in PID control loops, a bias term and an acceleration term are also used. The bias terms is initialized to the value of thrust that approximately negates the effects of gravity and keeps the accumulator balanced. The acceleration term, used to counteract short term acceleration of the quadrotor, makes use of the output of the accelerometer instead of the output of the Kalman filter since the direct measurement is less prone to noise.

B. Pose Control

Control of the quadrotor along the horizontal plane is achieved by using feedback from the scanning laser rangefinder and the IMU. The laser scans are processed onboard using the HectorSLAM method [13]. This method constructs a pixelated representation of a two-dimensional floor

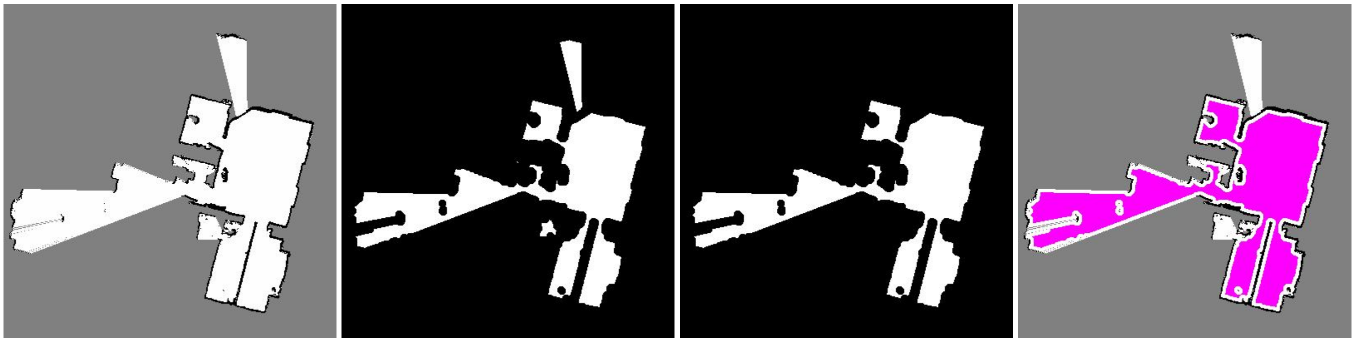

(a) Original Map (b) Eroded Map (c) Largest Conn. Comp. (d) Navigable Space

Figure 6: The process of determining the free space for path planning. a) The original map from HectorSLAM including labels for unknown space (gray), space occupied by an obstacle (black), and unoccupied space (white). b) The unoccupied space after it has been eroded. c) The unoccupied space after unconnected blobs are removed. d) The navigable space overlaid on the original map.

plan by assigning each pixel to either a filled space, an empty space, or an unobserved space. A gradient-based method is used to quickly approximate the results of the iterative closest point (ICP) algorithm in order to perform accelerated scan matching and, as a result, localize the quadrotor within the map. While the method does not natively include a method for loop closure, it has been found to perform sufficiently well for small to moderate workspaces.

The onboard scanning laser rangefinder used by the proposed system is the Hokuyo UTM-30LX, which is configured to scan a $180°$ area in front of the quadrotor at a resolution of $0.25°$ and a rate of 40 Hz. The onboard CPU processes the scans in real-time, i.e., the map is updated and the quadrotor position is calculated before the next scan becomes available.

The control strategy used to achieve stability in the horizontal plane is identical to that given in [6], except that instead of using external tracking, the proposed system uses onboard localization.

C. Path Planning

In order to allow the quadrotor to scan the area for passive RFID tags, a series of map processing stages have been developed along with a wall-following algorithm. Due to the orthogonality of the walls, floors and ceilings in typical indoor environments, path planning can be reduced to two dimensions. The map is produced by HectorSLAM by processing data from the scanning laser rangefinder and is used to determine both the navigable space and the desired path. As seen in Figure 6a, the map includes three kinds of labels: unoccupied space, space occupied by obstacles, and unknown space. Essentially, if the scanning laser rangefinder records both the distance and direction to an obstacle, the coordinates of the obstacle are recorded as occupied space. At the same time, it is observed that the space between the scanner and the obstacle is unoccupied. All other spaces, including those that are occluded by obstacles or outside the range of the scanner, are designated as unknown.

Erosion is then used to determine the navigable space of the quadrotor to prevent collisions [14]. When the unoccupied space is eroded by a kernel with a diameter that is slightly larger the radius of the Ascending Technologies Pelican, the quadrotor's centroid can exist in the resulting space of coordinates. The process of erosion often produces a map with unconnected blobs. Since there is no navigable path that allows the quadrotor to travel to those spaces, only the blob in which the quadrotor resides is kept for the purposes of path planning. This process can be seen in Figures 6b, 6c, and 6d.

Once the navigable space has been defined, path planning begins. The position goal is assigned to the edge of the free space that is closest to the current position, with the orientation pointing towards the nearest occupied space, i.e., orthogonal to the wall. Once the quadrotor achieves a position that is within 10 cm of the current goal, a new goal position is defined along the border of the free space that is counter clockwise from the previous goal. Again, the orientation of the quadrotor is such that it always faces the nearest occupied space. This allows the RFID reader to be oriented properly to scan the occupied spaces. The process defined above is repeated until the quadrotor has scanned all of the occupied space.

D. Passive RFID Inventorying

The RFID reader used for this study was a SkyeModule M9. The module is capable of reading transponders based on the EPC Class1 Gen1, ISO 18000-6B, and ISO18000-6C tag protocols. It works in the ultra-high frequency (862-955 MHz) band which, when compared to high frequency and low frequency RFID tags, achieves a larger read range [15]. The module has a maximum transmit power of 27 dBm and a weight of 11 grams. Read range can vary depending on the antenna, the type of tags used, and the environment. Multiple tags were used in the various stages of testing including Omron 1x3" and Alien 2006 1800064.

IV. Results

There are several necessary components that allow the proposed system to perform automated RFID inventorying. For the quadrotor to fly autonomously, it must be capable of simultaneously mapping the space, localizing itself within that space, and performing flight control in order to maintain stable movement and positioning. Additionally, the RFID reader attached to the MAV must be able to reliably read passive RFID tags arranged within the space. The following sections study the performance of the individual components and verify the system's ability to autonomously perform RFID inventorying.

A. Autonomous Flight Stabilization

To evaluate the control method used for flight stabilization, the position goal was set to $X = 0$, $Y = 0$, $Z = 1.5$ meters (1.5 meters above ground at the origin of the coordinate system) and the quadrotor was programed to hover in place for 2 minutes. Figure 7 provides both AprilTag and onboard tracking for the experiment. The accuracy of the onboard tracking is presented in Table I, treating AprilTag as the ground truth. As expected, the X and Y onboard position tracking is close to AprilTag tracking, since it uses real-time HectorSLAM scan matching. Perhaps more surprising is the accuracy of the height estimation using Kalman filtering of the sonar and IMU data. It achieves a mean absolute error of 2.6882 cm, improving upon a mean absolute error of 2.8622 cm achieved when using sonar by itself. More importantly, using the predictive Kalman filter allows the quadrotor to dynamically adapt to changes in air pressure and fluctuations in thrust more quickly.

Table II presents statistics related to the achieved stability of the quadrotor. The results demonstrate that the quadrotor is effectively able to maintain its position within approximately 10 cm of the goal. It is expected that this level of stability should make it suitable for safe and effective operation in common indoor environments.

Table I: Mean error measures (in centimeters) for onboard positioning when compared to AprilTag motion capture.

	X	Y	Z
Mean Error	0.0177	0.0362	-0.0802
Mean Absolute Error	1.8970	0.8863	2.6882
Root Mean Squared Error	2.3705	1.1547	3.5219

Table II: Mean error (in centimeters) for two minute hovering experiment where the quadrotor was programmed to maintain its position at $X = 0$, $Y = 0$, $Z = 1.5$ meters.

	X	Y	Z
Mean Error	2.8104	6.9163	0.0318
Mean Absolute Error	6.1272	7.8965	7.3344
Root Mean Squared Error	7.9844	9.1966	9.3140

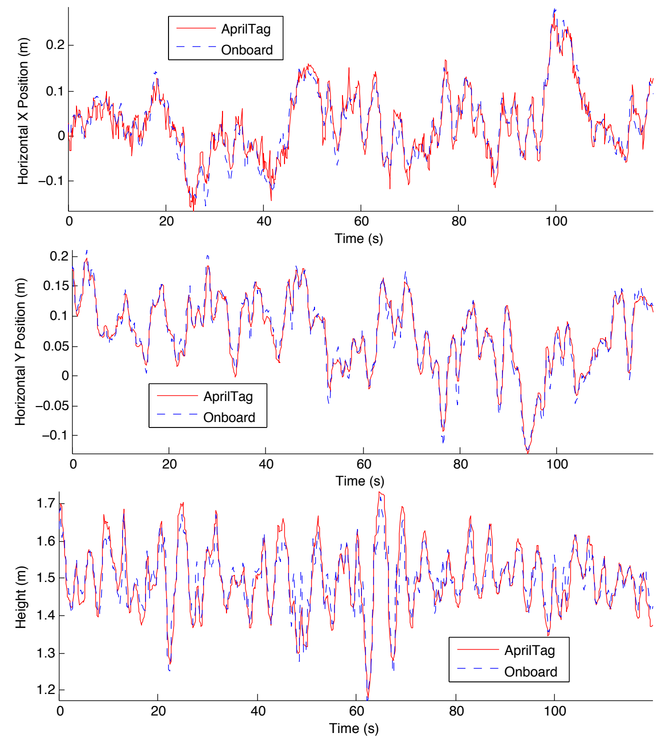

Figure 7: Position tracking using both AprilTag tracking and onboard Kalman filter estimation. The top illustrates the X position, the middle illustrates the Y position, and the bottom illustrates the height (Z position).

B. RFID Range

To empirically determine the range of Skyemodule M9, measurements were obtained to determine the maximum read range of the RFID reader from different directions. The five different directions included 0° (fronto-parallel), 45° up and down, and 45° right and left. When reading tags that are at 0°, the maximum read range was 119 cm. When reading tags at 45°, the read range averaged 63 cm, and when offset 45° in the vertical axis the read range averaged 112 cm.

The results demonstrate that the Skymodule M9 is capable of performing RFID inventorying from a relatively large distance and without needing to be oriented toward each passive RFID tag. The proposed MAV system takes advantage of this robustness in order to scan a large area with a relatively simple path-planning technique.

C. Autonomous RFID Inventorying

To test the system's ability to autonomously navigate the space and perform RFID inventorying, a set of three passive RFID tags were placed on three walls of a room with approximately a 3×4 meter floor space. The quadrotor was placed on the floor in the middle of the space prior to launch. At launch, the quadrotor increases the thrust until onboard altitude sensing determines that it has reached the desired height. For the experiment, the desired height was arbitrarily chosen to be 1 meter. While launching, the quadrotor is stabilizing its position horizontally in the room using HectorSLAM and feedback control. Once the desired height has been achieved, the quadrotor spins 360° while maintaining its horizontal position in order to scan all viewable walls and obstacles from the original position in the space.

Once the quadrotor has launched and scanned the viewable area, path planning proceeds as described in Section III-C. Figure 8 illustrates the map generated by the quadrotor, the path taken, and the position of the RFID tags. Three separate trials were performed to validate automated RFID inventorying. In each trial, the system was able to read all three passive RFID tags that were placed within the space.

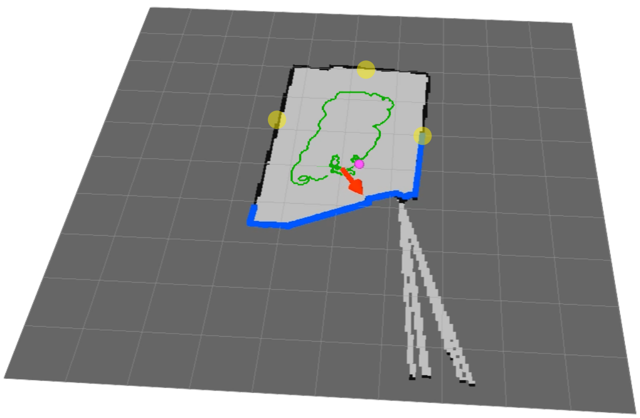

Figure 8: Map generated by the proposed system during automated RFID inventorying. The map illustrates the unobserved space (dark gray), observed empty space (light gray), walls (black), currently observed walls (blue), path (green), quadrotor position and orientation (red arrow), current position goal (magenta), and RFID tags (yellow).

V. Conclusion

It has been demonstrated that the proposed method is capable of performing automated indoor flight and RFID inventorying using a combination of onboard sensing, state estimation, feedback control, and path planning. Unlike many comparable MAV systems, the proposed system does not rely on a pre-generated map or external tracking for positioning and navigation. Experimental results show that the method presented for onboard positioning achieves a level of stability necessary for collision-free indoor flight. In addition, all experiments performed using the proposed path planning algorithm the onboard RFID reader show that the quadrotor is capable of automated inventorying without any knowledge of the location of the passive RFID tags.

Future work includes incorporating a method to avoid obstacles that lie below the hovering plane of the quadrotor. Possible solutions include generating a layered 3D map of the environment or including an upward facing ultrasonic depth sensor and using the IMU to select the most reliable measurement. Since the platform also includes a pair of cameras in a stereo configuration, they could also be used for 3D reconstruction of the environment using stereo matching for obstacle avoidance. Also, to assist loop closure for the indoor maps produced by SLAM, it may be possible to use the uniquely identifiable RFID tags.

References

[1] S. Shen, N. Michael, and V. Kumar, "Autonomous indoor 3D exploration with a micro-aerial vehicle," in *2012 IEEE International Conference on Robotics and Automation (ICRA)*, pp. 9–15, May 2012.

[2] M. Achtelik, A. Bachrach, R. He, S. Prentice, and N. Roy, "Autonomous navigation and exploration of a quadrotor helicopter in GPS-denied indoor environments," *First Symposium on Indoor Flight*, July 2009.

[3] S. Bouabdallah and R. Siegwart, "Full control of a quadrotor," in *IEEE/RSJ International Conference on Intelligent Robots and Systems, 2007. IROS 2007*, pp. 153–158, Oct. 2007.

[4] M. Bangura and R. Mahony, "Nonlinear dynamic modeling for high performance control of a quadrotor," in *Australasian Conference on Robotics and Automation*, pp. 1–10, 2012.

[5] P. Pounds, R. Mahony, and J. Gresham, "Towards dynamically favourable quad-rotor aerial robots," in *In Proc. of Australasian Conference on Robotics and Automation*, 2004.

[6] D. Gurdan, J. Stumpf, M. Achtelik, K.-M. Doth, G. Hirzinger, and D. Rus, "Energy-efficient autonomous four-rotor flying robot controlled at 1 kHz," in *2007 IEEE International Conference on Robotics and Automation*, pp. 361–366, Apr. 2007.

[7] D. Mellinger, N. Michael, and V. Kumar, "Trajectory generation and control for precise aggressive maneuvers with quadrotors," *The International Journal of Robotics Research*, vol. 31, pp. 664–674, Apr. 2012.

[8] S. Grzonka, G. Grisetti, and W. Burgard, "A fully autonomous indoor quadrotor," *IEEE Transactions on Robotics*, vol. 28, pp. 90–100, Feb. 2012.

[9] S. Shen, N. Michael, and V. Kumar, "Autonomous multi-floor indoor navigation with a computationally constrained MAV," in *2011 IEEE International Conference on Robotics and Automation (ICRA)*, pp. 20–25, May 2011.

[10] S. Shen, N. Michael, and V. Kumar, "Obtaining liftoff indoors: Autonomous navigation in confined indoor environments," *IEEE Robotics Automation Magazine*, vol. 20, pp. 40–48, Dec. 2013.

[11] F. Kendoul, "Survey of advances in guidance, navigation, and control of unmanned rotorcraft systems," *Journal of Field Robotics*, vol. 29, no. 2, p. 315âĂŞ378, 2012.

[12] E. Olson, "AprilTag: a robust and flexible visual fiducial system," in *2011 IEEE International Conference on Robotics and Automation (ICRA)*, pp. 3400–3407, May 2011.

[13] S. Kohlbrecher, O. Von Stryk, J. Meyer, and U. Klingauf, "A flexible and scalable SLAM system with full 3D motion estimation," in *2011 IEEE International Symposium on Safety, Security, and Rescue Robotics (SSRR)*, pp. 155–160, Nov. 2011.

[14] S. LaValle and J. Kuffner, J.J., "Randomized kinodynamic planning," in *1999 IEEE International Conference on Robotics and Automation, 1999. Proceedings*, vol. 1, pp. 473–479 vol.1, 1999.

[15] "SkyeModule m9 reference guide version 080527," tech. rep., Skyetek Inc., Westminster, CO, 2008.